Applied Surface Science 390 (2016) 346–349

Contents lists available at ScienceDirect

Applied Surface Science

journal homepage: www.elsevier.com/locate/apsusc

Time evolution of secondary electron emission and trapped charge accumulation in polyimide film under various primary electron irradiation currents

Bai-Peng Song[a], Run-Dong Zhou[a], Guo-Qiang Su[a], Hai-Bao Mu[a,*], Guan-Jun Zhang[a,*], Ren-An Bu[b]

[a] *State Key Laboratory of Electrical Insulation and Power Equipment, School of Electrical Engineering, Xi'an Jiaotong University, Xi'an, Shaanxi 710049, China*

[b] *School of Electronic and Information Engineering, Xi'an Jiaotong University, Xi'an, Shaanxi 710049, China*

ARTICLE INFO

Article history:
Received 2 June 2016
Accepted 30 July 2016
Available online 25 August 2016

Keywords:
Secondary electron emission
Trapped charges accumulation
Capture cross section

ABSTRACT

Time-resolved evolution of secondary electron emission and trapped charge accumulation in polyimide film is investigated during two interval electrons bombardment, derived from the measurement of displacement current and secondary current via a hemispherical detector with the shielded grid. Under various irradiation current, secondary electron yield (SEY σ) at a certain injected energy decreases exponentially from initial amplitude σ_0 to self-consistent steady value σ^∞ close to 0.93. The time constant τ of charging process is characterized as a function of incident current I_p, and the results indicate that the formula $I_p \times \tau$ is fitted by a hyperbolical law. The influence of I_p on the amount of trapped charge is studied and no significant change in its saturation value is observed. The evolution of SEY σ and trapped charge is dependent on incident dose Q_p but not the incident rate I_p. Furthermore, the trap density and capture cross section are discussed.

1. Introduction

Electron irradiation on dielectrics leads to secondary electron emission and charge trapping, and this is of considerable interest in many scientific fields and applied facilities. Secondary electrons and trapped charges characterize the insulation properties of materials and have significant influences on electro-vacuum devices [1], high power pulse equipment [2,3], spacecraft charging phenomena [4,5], particle accelerators [6], *etc*. The induced multipactor effect can produce electron avalanche resulting in surface flashover and breakdown, disturb microwave communication and overheat facility components. Moreover, secondary electrons emission and surface charges play a key role in scanning electron microscopy (SEM), because the charged surface can degrade the quality of SEM images and deteriorate the precision of critical dimension metrology [7,8].

Electron beam interaction on a dielectric material consists of complicated dynamic processes of internal charge transport [8–16]. Primary electrons (PEs) inject the sample, and lose incident energies as a function of penetration depth and incident angles by elastic and inelastic scattering and collisions. During this process, inner secondary electrons are produced and then move up to the surface or to the ground, but only backscattered electrons (BSEs) and a fraction of secondary electrons (SEs) with sufficient kinetic energy can surmount the potential barrier into vacuum, and the rest are trapped in the sample. The accumulation of trapped charges establishes internal electric field, affecting injected electrons trajectories and charging energy loss. The electron and hole traps are accounted for trapped charges, and the primary electrons excite and stimulate electron-hole pairs. These traps will undergo scattering, drift, diffusion and recombination, and finally affect the surface voltage attenuation and charge transport, resulting in the change of external SEY and reaching the self-consistent steady state [11–14,17].

As for close relationship of secondary electron emission and trapped charges, Jacques Cazaux has constructively promoted to analyze complicated mechanisms involved in charging and discharging of insulators investigated by SEM [8,13]. H. J. Fitting et al. study the evolution of start-up and decay of SEY, spatial distributions of currents, internal field and surface potential by establishing electron-hole flight-drift model [11,12]. M. Belhaj et al. use novel Kelvin probe (KP method) to study incident electron influence on

* Corresponding authors.
E-mail addresses: haibaomu@xjtu.edu.cn (H.-B. Mu), gjzhang@xjtu.edu.cn (G.-J. Zhang).

http://dx.doi.org/10.1016/j.apsusc.2016.07.179
0169-4332/

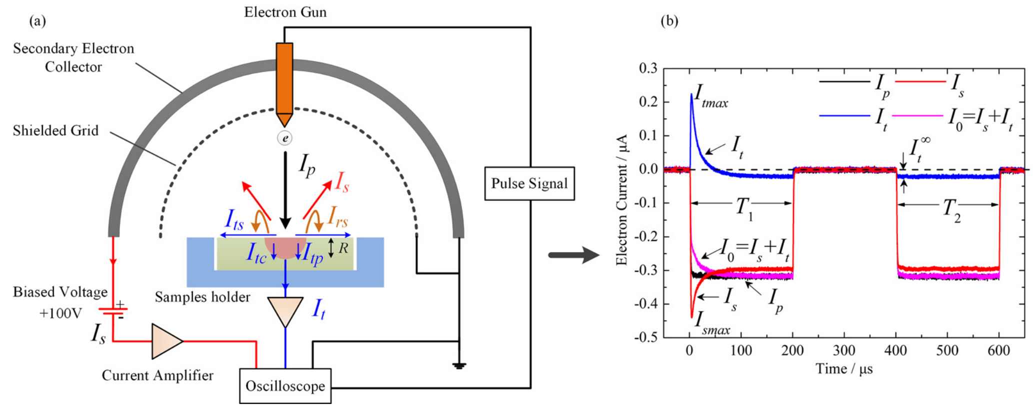

Fig. 1. Schematic diagram of secondary electron emission measurement system. I_p, I_s, and I_t are incident primary current, secondary current (including SEs current and BSEs current), and displacement current. I_{ts}, I_{tc}, I_{tp} and I_{rs} represent surface leakage current, bulk conduction current, polarization current and returned SEs current respectively. R is the inelastic mean free path of incident electrons. The right diagram (b) is the typical waveforms in two continuous plus periods.

the SEY yield, and concluded that recombination of the generated secondary electrons with accumulated holes leads to decrease of mean free paths and decay of SEY [14,16]. Moreover, S. Fakhfakh [9], G. Moya [17], G. Chen [18], H. B. Zhang [19], A. Hadjadj [20] and other researchers devote their efforts to investigate experimental measurements and theoretical modeling of electron emission and charging formation. However, the evolution of charging behavior under electron irradiation is still very complex to describe, and the understanding of the formation, accumulation and the stability of charges during and after primary electrons need further investigation.

In this article, we investigate time-resolved evolution of secondary electron emission and trapped charges accumulation. The aim of the study is to figure out the dominant characteristics of dynamic processes from the initial value to self-consistent steady state.

2. Experimental method

The measurement schematic diagram of total secondary electron emission yield (SEY σ) is described in Fig. 1(a). An electron gun (Kimball Physics, EGL-2022) of μs pulsing width is applied as the electron source. The target sample is 50 μm-thickness polyimide (PI) film, widely used in many electrical devices, spacecraft, pulsed power equipment. The hemispherical detector with the grid is used to collect SEs, and this collection method has been proved to be accurate and effective by Patino et al. [21], Thomson and Dennison group [22], *etc*. The hemispherical detector with almost 180°collecting angle is biased to +100 V positive voltage V_{biased}, equipped with a shielded grid (connected to ground during the measurement). This shielded grid is aimed to provide a uniform electric field and reduce unwanted influences of the biased voltage on the primary electrons trajectories. This is because that PEs motion are sensitive to the biased voltage V_{biased}, especially in the case of low incident energy E_p (*e.g.* when E_p is lower than eV_{biased}), and the biased electric field can diffuse the electrons beam, so that a fraction of electrons may be directly attracted to the collector before impacting the sample [23]. As for the gird, the electron passing rate is calculated by geometrical area ratio and verified by experimental measurements. The primary current I_p, secondary current I_s and induced current I_t are amplified by Femto DLPCA-200 and stored in the Tektronix DPO 4034 oscilloscope. The whole instrument is working at room temperature and below 5.0×10^{-4} Pa.

I_p is measured by the Faraday cup, I_s contains the true SEs and BSEs, and sample to ground current I_t is sum of four components, including returned SEs current I_{rs}, surface leakage current I_{ts}, bulk conduction current I_{tc}, and polarization current I_{tp}. I_{rs} is the current of SEs returning to the surface because of surface positive potential [19]. I_{ts}, I_{tc} are characterized by sample bulk volume electrical resistance and surface leakage conductivity. I_{tp} is subjected to scattering and transport of internal electrons and holes, including their trapping, drift, recombination, and detrapping. For studying the time-dependent initiation and decay of secondary electrons emission, two continuous irradiation pluses are used to analyze the evolution [24], as given in Fig. 1(b). The pulse width is set as 200 μs and the interval is also 200 μs at incident energy E_p = 400 eV (when $\sigma > 1$).

3. Results and discussion

3.1. Time constant τ under various electron irradiation currents

During the first pulse period, I_t and I_s are followed by the same attenuation tendency and both decreased from I_{tmax}, I_{smax} to steady states I_t^{∞} and I_s^{∞}, fitted by an exponential decay law $I(t) = I^{\infty} + (I_{t=0} - I^{\infty})\exp(-t/\tau)$, here τ is the time constant. The attenuation phenomena can be explained by combined influences of internal trapped charge and electrical field[12–14]. It must be pointed out that during the initiation of the first irradiation, $I_s + I_t < I_p$ until they attenuate to the steady state, $I_s + I_t = I_p$. The possible reason is that some SEs are attracted by positive electrical field to the surface[19]. In the second irradiation, I_t and I_s are both steady, equal to steady values of the first pulse, and it indicates that 200 μs interval relaxation does not induce migration or drift of trapped charges, and thus surface potential is almost unchanged. The equation of $I_s + I_t = I_p$ is always valid in the second irradiation.

The time constant τ defines the charging process rate and is influenced by the incident primary currents. Fig. 2 shows the displacement current I_t under various incident currents I_p at E_p = 400 eV. It is obvious that the higher incident current leads to lower time consumed to build up the self-consistent steady state: $\tau_1 = (6.77 \pm 0.21) \times 10^{-5}$ s of I_p = 60 nA, $\tau_2 = (5.32 \pm 0.17) \times 10^{-5}$ s of I_p = 78 nA, $\tau_3 = (2.24 \pm 0.07) \times 10^{-5}$ s of I_p = 195 nA, $\tau_4 = (1.38 \pm 0.02) \times 10^{-5}$ s of I_p = 315 nA. What's more, the steady states of normalized I_t^{∞}/I_p are almost the same, meaning that $(I_{rs}^{\infty} + I_{ts}^{\infty} + I_{tc}^{\infty})/I_p \approx 7\%$. It means that during the saturation period, I_{rs}^{∞}, I_{ts}^{∞} and I_{tc}^{∞} are not dependent on incident primary currents but characterized by surface potential, sample surface and bulk volume conductivity.

Measurements of time constant τ are repeated under various incident currents, and the relationship of τ and I_p is shown in Fig. 2 inset. It is obvious that experimental data are matched very